DRPEER: A Motif in the Extracellular Vestibule Conferring High Ca^{2+} Flux Rates in NMDA Receptor Channels

Junryo Watanabe,[2] Christine Beck,[3] Thomas Kuner,[3,4] Louis S. Premkumar,[5] and Lonnie P. Wollmuth[1]

[1]Department of Neurobiology and Behavior and [2]Graduate Program in Neurobiology and Behavior, State University of New York at Stony Brook, Stony Brook, New York 11794-5230, [3]Abteilung Molekulare Neurobiologie and [4]Zellphysiologie, Max-Planck-Institut für medizinische Forschung, D-69120 Heidelberg, Germany, and [5]Department of Pharmacology, Southern Illinois University School of Medicine, Springfield, Illinois 62702

The high flux rate of Ca^{2+} through NMDA receptor (NMDAR) channels is critical for their biological function and may depend on a Ca^{2+} binding site in the extracellular vestibule. We screened substitutions of hydrophilic residues exposed in the vestibule and identified a cluster of charged residues and a proline, the DRPEER motif, positioned C terminal to M3, that is unique to the NR1 subunit. Charge neutralization or conversion of residues in DRPEER altered fractional Ca^{2+} currents in a manner consistent with its forming a binding site for Ca^{2+}. Similarly, in a mutant channel in which all of the negative charges are neutralized (ARPAAR), the block by extracellular Ca^{2+} of single-channel current amplitudes is attenuated. In these same channels, the block by extracellular Mg^{2+} is unaffected. DRPEER is located extracellularly, and its contribution to Ca^{2+} influx is distinct from that of the narrow constriction. We conclude that key residues in DRPEER, acting as an external binding site for Ca^{2+}, along with a conserved asparagine in the M3 segment proper, contribute to the high fractional Ca^{2+} currents in these channels under physiological conditions. Therefore, these domains represent critical molecular determinants of NMDAR function in synaptic physiology.

Key words: glutamate receptor; fractional Ca^{2+} currents; Ca^{2+} permeability; extracellular vestibule; synaptic physiology; Ca^{2+} binding site

Excitatory neurotransmission in the brain is predominantly mediated by ionotropic glutamate receptors (GluRs). Ca^{2+} influx through GluR channels, primarily the NMDA receptor (NMDAR) subtype, is the major synaptically controlled mechanism of Ca^{2+} influx and mediates many of the biological functions of their activation, including their proposed role in changes in synaptic efficacy, gene expression, and development of cellular connections (Dingledine et al., 1999). Excessive Ca^{2+} influx through these receptors also contributes to the cell death associated with a number of neurological diseases, including hypoxia/ischemia, hypoglycemia, epilepsy, and chronic neurodegenerative disorders (Lee et al., 1999). Despite the critical nature of this process, the molecular basis by which NMDARs allow Ca^{2+} entry into the cell is poorly defined.

All NMDAR isoforms are, with quantitative differences, highly permeable to Ca^{2+} and allow an approximately threefold to fourfold greater influx of Ca^{2+} than Ca^{2+}-permeable AMPA receptor (AMPAR) channels (Burnashev et al., 1995; Wollmuth and Sakmann, 1998). In GluRs, the degree of Ca^{2+} influx depends on the amino acid residue occupying a functionally critical position in the M2 loop, commonly known as the Q/R site in AMPARs and the N site in NMDARs (Burnashev, 1996). Still, the composition of the Q/R/N site alone does not mediate the difference in Ca^{2+} flux between the GluR subtypes, because mutant AMPAR channels containing an asparagine at the Q/R site retain a low Ca^{2+} influx (Wollmuth and Sakmann, 1998). In addition, biophysical evidence has suggested that the mechanism of Ca^{2+} influx in NMDAR channels depends on multiple sites in the pore for Ca^{2+} (Premkumar and Auerbach, 1996; Sharma and Stevens, 1996). As a working definition, we distinguish these multiple components into "deep" and "external" sites for Ca^{2+}, corresponding to regions central in the pore and at the external mouth of the channel, respectively. Residues at the narrow constriction of the channel, which include the NR1 N site asparagine (Wollmuth et al., 1996), may form part of the deep site (Burnashev et al., 1992; Premkumar et al., 1997), but the structural elements forming the external site are unknown. This distinction is not simply a biophysical issue: The putative external site appears to be the critical determinant of the high Ca^{2+} flux rates in NMDAR channels (Premkumar and Auerbach, 1996; Sharma and Stevens, 1996) and may be absent in AMPAR subunits (Wollmuth and Sakmann, 1998).

Determinants of the extracellular vestibule, as contributed by the NR1 subunit, have been identified (Beck et al., 1999). Therefore, we screened charged and polar residues in the extracellular vestibule and identified a cluster of charged residues and a proline, the DRPEER motif, located C terminal to M3. This motif is unique to the NR1 subunit. Based on measurements of fractional Ca^{2+} currents under physiological conditions, DRPEER represents a key determinant of the high Ca^{2+} influx mediated by NMDAR channels.

MATERIALS AND METHODS

Molecular biology. All experiments were performed with previously described expression constructs for wild-type NR1, NR2A, and NR2C NMDAR subunits (Kuner et al., 1996; Wollmuth et al., 1996). Unless otherwise noted, channels were expressed transiently in human embry-

Received May 2, 2002; revised Sept. 24, 2002; accepted Sept. 26, 2002.

This work was supported by National Institutes of Health Grant RO1 NS39102 and a Sinsheimer Scholars Award to L.P.W. We thank Drs. C. Jatzke and G. Matthews for their comments on this manuscript and M. Kaiser, S. Grünewald, L. Rooney, and G. I. Robinson for technical assistance.

Correspondence should be addressed to Dr. Lonnie P. Wollmuth, Department of Neurobiology and Behavior, State University of New York at Stony Brook, Stony Brook, NY 11794-5230. E-mail: lwollmuth@notes1.cc.sunysb.edu.

Copyright © 2002 Society for Neuroscience 0270-6474/02/2210209-08$15.00/0

onic kidney 293 (HEK 293) cells using Lipofectamine 2000 (Invitrogen, Rockville, MD). Alternatively, NMDAR subunits were injected into *Xenopus* oocytes (Wollmuth et al., 1996).

Site-directed mutations were generated either by PCR-based methods or by using the QuickChange Site-Directed Mutagenesis kit (Stratagene, La Jolla, CA). Mutations were initially generated in clones present in a pSP64T-derived vector (Kuner et al., 1996; Wollmuth et al., 1996). Appropriate fragments containing the mutation were then subcloned into the corresponding wild-type construct present in either the pSP vector or the eukaryotic expression vector pRK. All constructs were sequenced over the entire length of the replaced fragment. NR1 mutants were expressed together with wild-type NR2A or vice versa. Current amplitudes in all mutant channels were comparable with those in wild type, with two exceptions. NR1–NR2A(D641R) showed very small current amplitudes (~40 pA at −60 mV), and no glutamate activated currents could be detected in cells transfected with NR1–NR2A(N629A) (see Fig. 1).

Current recordings and data analysis. Whole-cell currents were recorded at room temperature (20–23°C) using an EPC-9 amplifier (HEKA Elektronik, Lambrecht, Germany) (Jatzke et al., 2002). The intracellular solution contained (in mM): 140 KCl, 10 HEPES, 10 EGTA, pH 7.2, and KOH. Our standard extracellular solution contained (in mM): 140 NaCl, 10 HEPES, pH 7.2, and NaOH, to which Ca^{2+} or Mg^{2+} was added. External solutions were applied using a piezo-driven double-barreled application system: one barrel contained the external solution plus 50 μM glycine and the other barrel the same solution but with 200 μM glutamate added. Unless otherwise noted, all chemicals were obtained from Sigma Aldrich Inc. (St. Louis, MO).

Fractional Ca^{2+} currents. Fura-2 (1 mM; Molecular Probes, Eugene, OR) was loaded into HEK 293 cells via the patch pipette to measure the fraction of the total current carried by Ca^{2+} (Neher, 1995; Jatzke et al., 2002). Fractional Ca^{2+} currents (P_f) were quantified using the following equation: P_f (%) = 100 × Q_{Ca}/Q_T, where Q_{Ca} and Q_T are the charge carried by Ca^{2+} and the total charge, respectively, during a defined time interval. In measuring P_f values, our intracellular solution contained (in mM): 140 KCl, 10 HEPES, 1 K_5·fura-2, pH 7.2, and KOH.

Ca^{2+} permeability. Changes in the reversal potential, ΔE_{rev}, were used as an index of Ca^{2+} permeability relative to that for Cs^+ (Wollmuth and Sakmann, 1998). Briefly, ΔE_{rev} for glutamate-activated currents was measured after replacing a Cs^+-based reference solution (140 mM CsCl, 10 mM HEPES, pH 7.2, and CsOH) with a solution in which CsCl was replaced by 1.8 mM Ca^{2+} and 140 mM *N*-methyl-D-glucamine (NMDG), pH 7.2, HCl. The pipette solution consisted of (in mM): 140 CsCl, 10 EGTA, 10 HEPES, pH 7.2, and CsOH. Peak current amplitudes, generated by voltage steps in 5 or 10 mV increments and corrected for junction potentials, were plotted against voltage and fitted with a fourth-order polynomial to determine the reversal or zero potential. ΔE_{rev} values were converted to P_{Ca}/P_{Cs} using the Lewis equation [Wollmuth and Sakmann (1998), their Eq. 8].

Single-channel recordings. Single-channel current recordings were made from outside-out patches isolated from *Xenopus* oocytes using an Axopatch 2B (Axon Instruments, Union City, CA). The extracellular solution contained (in mM): 100 NaCl, 2.5 KCl, 5 HEPES, 1.5 EGTA, pH 7.3, and NaOH. Patch pipettes were coated with Sylgard (Dow Corning, Midland, MI) and filled with a solution containing (in mM): 90 Na-gluconate, 10 NaCl, 2 ATP, 0.25 GTP, 10 BAPTA, 10 HEPES, pH 7.3, and NaOH. Currents were recorded with the filter set at 10 kHz, digitized at 94 kHz (VR-10B; InstruTech, Great Neck, NY), and stored on videotapes. For analysis, currents were filtered at 2.5 kHz (−3 dB, eight-pole Bessel filter; Warner Instrument Corp., Hamden, CT) and digitized at 5 kHz. Single-channel current amplitude and P_o were estimated from all-point current–amplitude histograms (software kindly provided by Michael Smith, Australian National University, Canberra, Australia) and fitted to Gaussian densities (Origin; Microcal Software Inc., Northampton, MA).

Substituted cysteine accessibility method. Wild-type (NR1–NR2C) or cysteine-substituted NR1 subunits (along with wild-type NR2C) were injected into *Xenopus* oocytes (Sobolevsky et al., 2002). We used the NR2C rather than the NR2A subunit for these experiments because NR1–NR2C channels do not show any apparent desensitization (Krupp et al., 1996). Given the slow solution exchange rate in the whole-cell mode for *Xenopus* oocytes, this lack of desensitization simplifies data analysis and interpretation. The extracellular solution contained (in mM): 115 NaCl, 2.5 KCl, 0.18 $CaCl_2$, 10 HEPES, pH 7.2, and NaOH. Accessibility was assayed using steady-state reactions (Sobolevsky et al., 2002). The percentages of change in current amplitudes were calculated as follows: % = $(1 - I_{post}/I_{pre}) \times 100$, where I_{pre} and I_{post} are the average current amplitudes recorded before and after the application of the methanethiosulfonate (MTS) reagent 2-aminoethyl-MTS (MTSEA) (2 mM) applied in the continuous presence of glutamate. MTSEA was obtained from Toronto Research Chemicals (Toronto, Ontario, Canada).

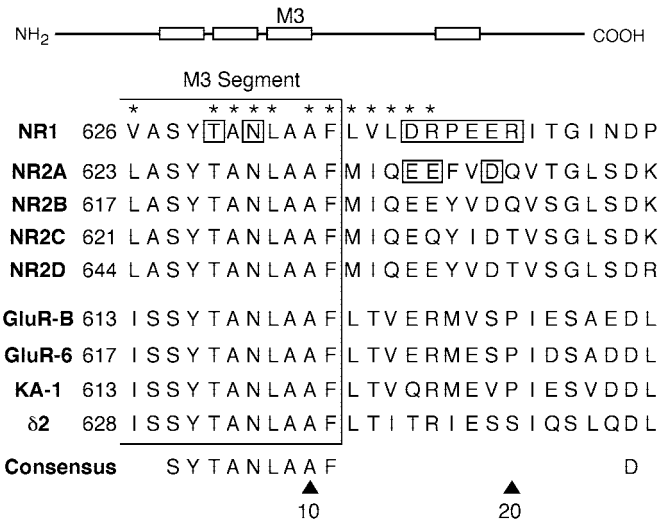

Figure 1. Sequence alignment of the C-terminal half and residues C terminal to the M3 segment in GluR subtypes. In this schematic drawing of GluR subunits, the four hydrophobic segments (M1–M4) are indicated as *open boxes*. The *enlarged region* shows a sequence alignment of amino acid residues on the C-terminal end and C terminal to M3. For clarity, only a subset of the receptor subtypes is shown (the region is highly conserved within subunits of the same subtype). The *sequence numbers* on the *left* are for the mature protein. For NR1, the *asterisks* indicate positions exposed to the water interface (Beck et al., 1999). The *boxed positions* for NR1 and NR2A were tested for their effects on Ca^{2+} permeability. The lower consensus sequence is found in all GluR subunits.

All curve fitting was done using Igor Pro (WaveMetrics Inc., Lake Oswego, OR). Results are reported below as means ± SEM and shown graphically as means ± 2 SEM. An ANOVA or a Student's *t* test was used to test for statistical differences. The Tukey test was used for multiple comparisons. Significance was assumed if $p < 0.05$.

RESULTS

The extracellular vestibule in NMDAR channels, as contributed by NR1, is formed by residues on the N-terminal side of M1 (pre-M1), the C-terminal part of M3, and the N-terminal part of M4 (Beck et al., 1999). To identify potential determinants of Ca^{2+} influx in the extracellular vestibule, we reasoned that Ca^{2+} would preferentially interact with negatively charged or polar residues in these domains. In mutant channels containing cysteine substitutions of such residues in pre-M1 or M4, Ca^{2+} permeability, measured using changes in reversal potentials and in 1.8 mM Ca^{2+}, was indistinguishable from that in wild type. In contrast, cysteine substitutions of such residues in the M3 segment did alter Ca^{2+} permeability (data not shown) [Beck et al. (1999), their Fig. 6]. Based on these observations, we focused on M3 and regions C terminal to it to identify determinants of Ca^{2+} influx. We also assumed that key external determinants would be absent in AMPAR subunits.

An NR1-specific motif C terminal to M3

Figure 1 compares the amino acid sequences of M3 and regions C terminal to it in selected GluR subunits. The C-terminal part of M3 (positions 1–11 in the alignment) is highly conserved across the subunits. For NR1, it does contain two polar residues that are

exposed, a threonine at position 5 (T630) and an asparagine at position 7 (N632). However, these residues are part of SYTANLAAF, the most highly conserved motif in GluRs; therefore, they represent poor candidates for a unique external site. In contrast, a sequence divergence occurs C terminal to M3, with two notable differences. First, a negatively charged glutamate (E) is present at position 16 in all NR2 subunits except for NR2C, whereas in all other subunits this position is occupied by the positively charged arginine (R). However, this charge difference makes no contribution to Ca^{2+} influx (Fig. 2*C*). The second difference occurs between positions 17 and 20, where NR1 has a cluster of charged residues and a proline (PEER). Along with DR at positions 15 and 16, which is conserved to some extent across the subtypes, we call this region the DRPEER motif, and consider it a candidate for an external Ca^{2+} site because it is located externally, contains a cluster of negative charges, and is unique to NR1.

Substitutions of the DRPEER motif alter Ca^{2+} influx

Under physiological conditions, the current carried through NMDAR channels is a mixture of monovalent cations (Na^+ and K^+) and Ca^{2+}. Hence, measuring the fraction of the total current carried by Ca^{2+}, which can be accomplished using dye overload (Neher, 1995), directly quantifies Ca^{2+} influx under physiological conditions. This approach is also advantageous, especially relative to measuring Ca^{2+} permeability using reversal potentials, because it is model independent and can be used to characterize Ca^{2+} influx over a wide voltage range.

Figure 2*A* summarizes fractional Ca^{2+} current (P_f) measurements at −60 mV and in approximate physiological conditions in wild-type and mutant NR1–NR2A channels containing alanine substitutions of the DRPEER motif. For the wild-type channels, P_f values were, on average, 13.6 ± 0.2% ($n = 33$). In all mutant channels, except P642A (12.8 ± 0.3%; $n = 7$) and R645A (13.8 ± 0.3%; $n = 8$), P_f values were significantly different from those in the wild type. For neutralization of the negative charges, D640A (10.6 ± 0.2%; $n = 9$), E643A (10.9 ± 0.4%; $n = 9$), and E644A (11.7 ± 0.2%; $n = 8$), P_f values were significantly less than those in the wild type, whereas for the first positive charge, R641A (14.9 ± 0.4%; $n = 7$), they were significantly greater. We also generated a mutant NR1 subunit in which all of the negative charges in DRPEER were replaced by alanines [NR1(ARPAAR)]. In this mutant channel, P_f values (7.1 ± 0.2%; $n = 12$) were significantly less than those either in wild type or in channels containing the individual alanine substitutions. These results directly demonstrate the functional significance of DRPEER to the high Ca^{2+} influx these channels carry under physiological conditions.

Ca^{2+} permeability ratios, based on reversal potential measurements, are an additional means to characterize Ca^{2+} influx in GluR channels. Figure 2*B* shows average Ca^{2+} permeability ratios, measured relative to Cs^+ (P_{Ca}/P_{Cs}) and in 1.8 mM Ca^{2+}, for wild-type and mutant channels containing alanine substitutions of the DRPEER motif. For wild type, P_{Ca}/P_{Cs} was, on average, 6.4 ± 0.1 ($n = 8$). P_{Ca}/P_{Cs} was significantly different from that in wild type for all of the mutant channels except R645A (6.5 ± 0.1; $n = 3$). Neutralization of the negative charges significantly reduced P_{Ca}/P_{Cs} (D640A, 5.0 ± 0.15, $n = 4$; E643A, 5.5 ± 0.05, $n = 5$; E644A, 5.8 ± 0.05, $n = 4$), whereas neutralization of the positive charge at 641 (R641A) significantly increased it (7.1 ± 0.1, $n = 5$). The observed pattern of significant changes completely parallels that observed for P_f values, with the exception of P642A, which showed a significant difference for P_{Ca}/P_{Cs} (6.0 ± 0.1; $n = 3$) but not for P_f measurements. As for P_f values,

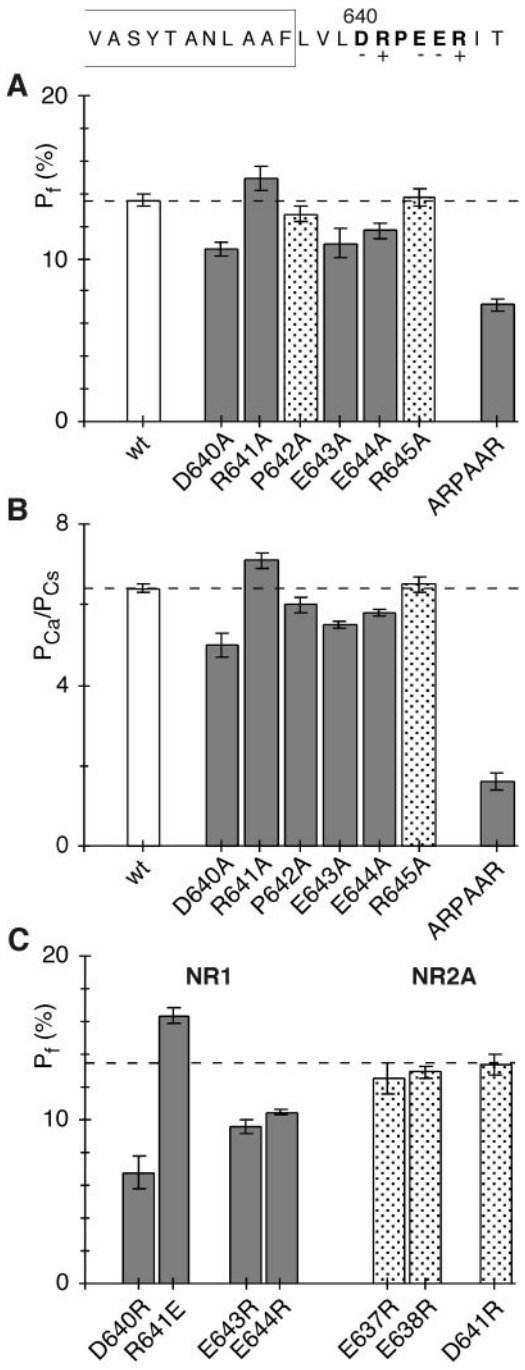

Figure 2. Fractional Ca^{2+} currents in wild-type and mutant NMDAR channels. *A*, Mean P_f values in wild-type (*wt*) and mutant NR1–NR2A channels containing alanine substitutions of the DRPEER motif. Cells were bathed in 143.5 mM NaCl and 1.8 mM $CaCl_2$. The holding potential (V) was −60 mV to the reversal potential (Jatzke et al., 2002). P_f values significantly different from those in wild type are shown as *gray bars*. *B*, Mean Ca^{2+} permeability ratios (P_{Ca}/P_{Cs}) in wt and mutant NR1–NR2A channels containing alanine substitutions of the DRPEER motif. P_{Ca}/P_{Cs} values were derived from changes in reversal potentials ongoing from a Cs^+-based reference solution to a solution in which CsCl was replaced by 1.8 mM Ca^{2+} and 140 mM NMDG (see Materials and Methods). P_{Ca}/P_{Cs} values significantly different from those in wild type are shown as *gray bars*. *C*, Mean P_f values in mutant channels containing oppositely charged substitutions of the DRPEER motif or of homologous positions in NR2A (see Fig. 1). Results are recorded and displayed as in *A*, except that the wild-type value is shown as a *dashed line*.

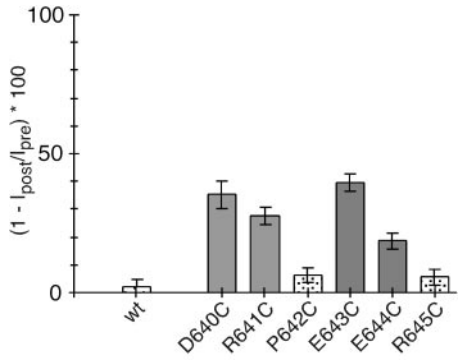

Figure 3. Accessibility of substituted cysteines in DRPEER to MTSEA. The mean percentage of change ($n > 5$) in current amplitudes measured before (I_{pre}) and after (I_{post}) exposure to MTSEA (2 mM, 60 sec application) (see Materials and Methods) is shown. MTS reagents were applied in the presence of glutamate. Statistically significant positions are shown as *gray bars*. *wt*, Wild type.

the triple mutant channel produced the strongest attenuation of P_{Ca}/P_{Cs} (1.6 ± 0.1; $n = 3$). These complementary experiments give strong support to the idea that a major function of the DRPEER motif is to contribute to the high Ca^{2+} influx mediated by NMDAR channels.

Neutralization of four of the charged residues in DRPEER altered fractional Ca^{2+} currents in a manner suggesting that it represents a binding site for Ca^{2+}. If Ca^{2+} interacts directly with DRPEER, opposite charge substitutions would magnify any functional change. As shown in Figure 2*C*, P_f values in D640R (6.8 ± 0.5%; $n = 7$) were significantly less than those in its corresponding alanine substitution, as were E643R (9.6 ± 0.2; $n = 6$) and E644R (10.5 ± 0.1; $n = 7$). Similarly, R641E (16.3 ± 0.2%; $n = 6$) was significantly greater than its corresponding alanine substitution. Therefore, these results support the idea that Ca^{2+} interacts directly with key residues in DRPEER.

C terminal to M3 in NR2A, three negative charges occupy positions homologous to those in the DRPEER motif (E637, E638, and D641) (Fig. 1). In channels containing oppositely charged substitutions of these residues, P_f values were not significantly different from those in wild type (Fig. 2*C*) (E637R, 12.6 ± 0.5%, $n = 5$; E638R, 12.9 ± 0.2%, $n = 7$; D641R, 13.3 ± 0.3%, $n = 5$). Thus, external determinants of Ca^{2+} influx in NMDAR channels are unique to NR1.

Key residues in DRPEER are exposed to the water interface based on the substituted cysteine accessibility method

To interact with Ca^{2+}, charged residues in DRPEER must be exposed to the water interface. To assay surface exposure, we used the substituted cysteine accessibility method (SCAM) (Karlin and Akabas, 1998; Sobolevsky et al., 2002), probing cysteine-substituted channels in the presence of glutamate with MTSEA. As shown in Figure 3, positions D640, R641, E643, and E644 showed persistent changes in current amplitudes after MTSEA treatment, whereas positions P642 and R645 did not. The interpretation of reactive and nonreactive positions is constrained by the assumptions of SCAM (Karlin and Akabas, 1998). Specifically, we assume that positions that are reactive are exposed to the water interface and line the lumen of the channel. We also assume that nonreactive positions are buried in the interior of the protein, particularly when adjacent positions are accessible to the reagents. Accordingly, the pattern of reactive positions is consistent with the idea that the DRPEER motif is located in the channel lumen and that key residues in it that affect Ca^{2+} influx are also exposed to the water interface. However, substitutions of R645 do not affect Ca^{2+} influx (Fig. 2), apparently reflecting the fact that it is not been exposed to the water interface (Fig. 3). However, it may be exposed but positioned too far externally to affect Ca^{2+} influx or current flow after MTS modification.

DRPEER contributes to the block by extracellular Ca^{2+}

NMDAR channels are highly permeable to Ca^{2+}, but paradoxically, currents are reduced in amplitude with added extracellular Ca^{2+} (Ascher and Nowak, 1988; Jahr and Stevens, 1993). Such a blocking action by a permeant ion is typically assumed to reflect binding. For NMDAR channels, the block by Ca^{2+}, which is essentially voltage independent, led to the proposal of an external

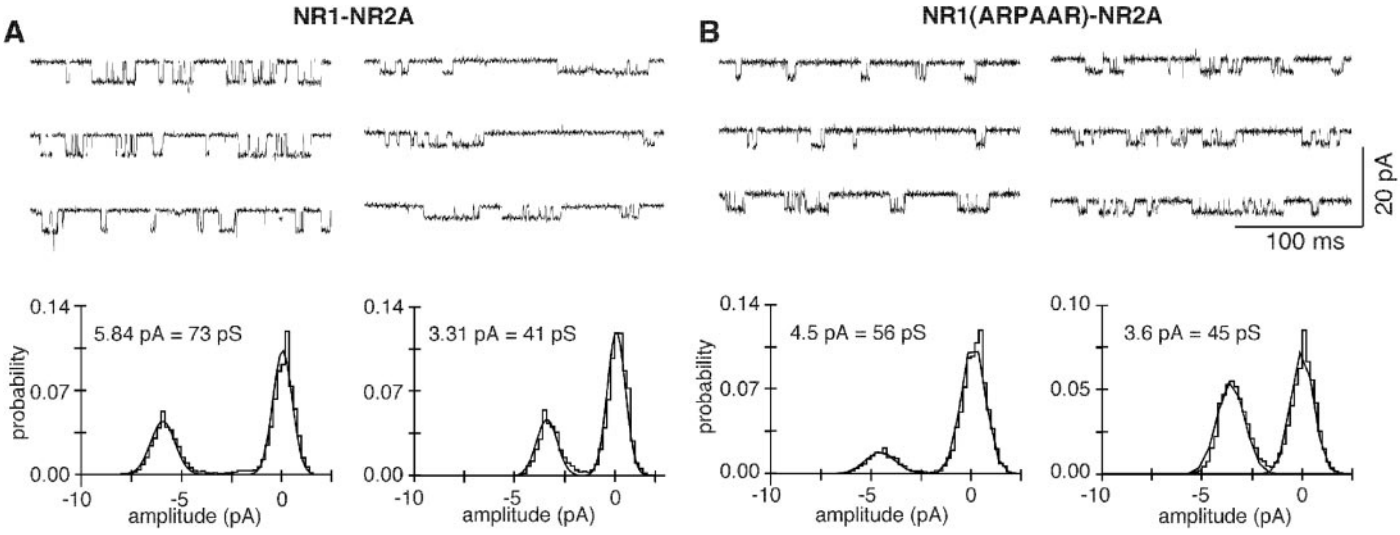

Figure 4. Block by Ca^{2+} in wild-type and mutant NMDAR channels. *A*, Single-channel currents at −80 mV in the absence (1.5 mM EGTA) (*left*) or presence (*right*) of 1 mM Ca^{2+}. *Traces* are from an outside-out patch isolated from a *Xenopus* oocyte expressing wild-type NR1–NR2A channels. *Bottom*, All-point amplitude histogram in the absence (*left*) or presence (*right*) of 1 mM Ca^{2+}. Continuous curves are maximum likelihood fits of Gaussian distributions. *B*, Same as *A*, except the oocyte was expressing NR1(ARPAAR)–NR2A.

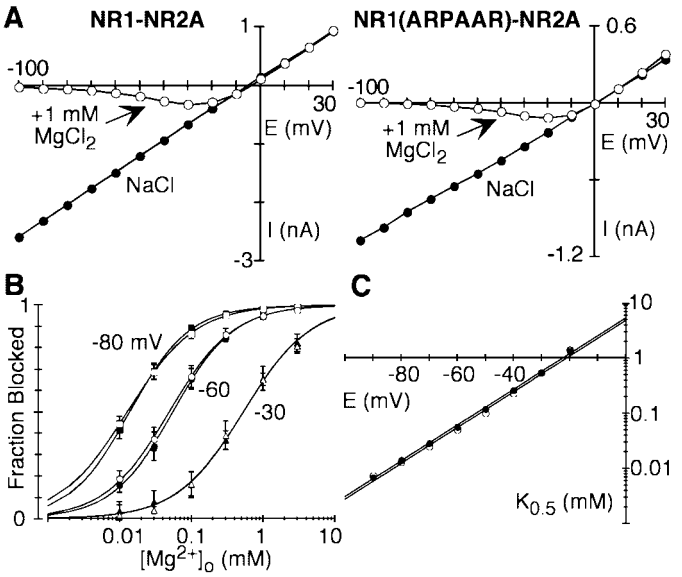

Figure 5. Extracellular Mg^{2+} block in wild-type and mutant NMDAR channels. *A*, Peak current–voltage relationship for glutamate-activated currents in wild-type or NR1(ARPAAR)–NR2A channels with NaCl externally either in the absence (●) or in the presence (○) of 1 mM Mg^{2+}. The control recording is an average of currents recorded before and after the Mg^{2+} exposure. *B*, Mean fraction blocked, $1 - I_B/I_0$ ($n > 5$ for each concentration), in the presence (I_B) or absence (I_0) of different Mg^{2+} concentrations at three potentials for wild-type (*solid symbols*) or ARPAAR (*open symbols*) channels. Continuous curves are fitted Langmuir isotherms $[1/(1 + K_{0.5}(E)/[Mg^{2+}]_o)]$, where $K_{0.5}(E)$ is the half block at any one potential and $[Mg^{2+}]_o$ is the external Mg^{2+} concentration. *C*, $K_{0.5}$ as a function of membrane potential, with the *straight line* indicating a linear equation fit from −90 to −20 mV, from which the half-block at 0 mV [$K_{0.5}$ (0 mV)] and the voltage dependence of the block (δ) were derived (Wollmuth et al., 1998a).

binding site for Ca^{2+} (Premkumar and Auerbach, 1996; Sharma and Stevens, 1996).

Figure 4 illustrates experiments showing that DRPEER represents a determinant of the block by extracellular Ca^{2+}. For wild-type NR1–NR2A channels, the single-channel conductance at −80 mV and in the absence of Ca^{2+} (1.5 mM EGTA) is ~73 pS (73 ± 1.4; $n = 6$) (Fig. 4*A*, *left*). In 1 mM free Ca^{2+} (Fig. 4*A*, *right*), this conductance is reduced to ~42 pS (42 ± 1.5; $n = 6$), consistent with Ca^{2+} blocking monovalent currents under these conditions by ~43%. NR1(ARPAAR)–NR2A channels (Fig. 4*B*), like wild type, show a single conductance level under all conditions that is ~56 pS (56 ± 1.2; $n = 7$) in the absence of Ca^{2+} (Fig. 4*B*, *left*). This value is significantly less than that in wild type, indicating that DRPEER contributes to monovalent fluxes. However, although Ca^{2+} (1 mM) (Fig. 4*B*, *right*) reduces the single-channel conductance to ~43 pS (43 ± 1.0; $n = 6$), the fractional block is only 24%, compared with 43% in wild type. This attenuation of the block strongly supports the idea that DRPEER represents an external Ca^{2+} binding site. The fact that the block is not completely eliminated by neutralization of DRPEER is not surprising, because the Ca^{2+} influx in NMDAR channels depends on multiple sites in the pore (see below). Nevertheless, as found for P_f values (Fig. 2*A*), DRPEER represents a determinant of this block process consistent with it contributing to the mechanism of Ca^{2+} influx in these channels. Ca^{2+} also enhances P_{open} in NR1(ARPAAR)–NR2A channels, an effect that we do not explore further here.

Table 1. Fractional Ca^{2+} currents (P_f) and Ca^{2+} permeability (P_{Ca}/P_{Cs}) in mutant NMDAR channels containing substitutions of the M2 loop or M3 segment

Subunit combination	P_{Ca}/P_{Cs}	*n*	P_f (%)	*n*
NR1–NR2A	6.4 ± 0.1	8	13.6 ± 0.2	33
NR1(N0Q)–NR2A	ND		7.8 ± 0.5*	5
NR1(N0G)–NR2A	1.5 ± 0.1*	5	7.8 ± 0.6*	4
NR1–NR2A(N0Q)	ND		13.7 ± 0.8	4
NR1–NR2A(N0G)	6.1 ± 0.1	6	12.8 ± 0.4	4
NR1–NR2A(N+1G)	2.9 ± 0.1*	4	8.8 ± 0.3*	7
NR1(T630C)–NR2A	6.2 ± 0.2	3	ND	
NR1(N632C)–NR2A	4.9 ± 0.1*	6	ND	
NR1(N632A)–NR2A	4.8 ± 0.1*	4	10.3 ± 0.2*	6

Values are shown as mean ± SEM and were measured as in Figure 2. The N0 and N+1 designation corresponds to the N sites (N598 in NR1 and N595 in NR2A) and to an adjacent asparagine (N596) in NR2A, respectively (Kuner et al., 1996). NR1(N0), NR2A(N0), and NR2A(N+1) are located in the M2 loop, whereas T630 and N632 are located in the M3 segment proper (Fig. 1). ND, Not determined.

*Significantly different from wild type.

DRPEER does not contribute to the mechanism of block by extracellular Mg^{2+}

Two physiological divalents, Ca^{2+} and Mg^{2+}, are critical to the function of NMDAR channels in synaptic physiology. In contrast to its effects on Ca^{2+} influx, neutralization of DRPEER had no effect on the voltage-dependent block by extracellular Mg^{2+} (Fig. 5*A*). Indeed, the extent of the block measured over a wide range of Mg^{2+} concentrations (0.01–3 mM) was indistinguishable at negative potentials (Fig. 5*B*). We used a Woodhull model to quantify the half-maximal block at 0 mV [$K_{0.5}$ (0 mV)] and its voltage dependence (δ) (Fig. 5*C*) (Wollmuth et al., 1998a). For wild-type, $K_{0.5}$ (0 mV) and δ were 5.2 ± 0.3 and 0.95 ± 0.02 mM, respectively. Indistinguishable results were obtained for ARPAAR channels (4.9 ± 0.6 and 0.97 ± 0.04 mM). Thus, in NMDAR channels, distinct domains are involved in determining the high Ca^{2+} influx and voltage-dependent block by Mg^{2+}.

Multiple determinants of Ca^{2+} influx in NMDAR channels

In NMDAR channels, the narrow constriction is located near the tip of the M2 loop and is formed by nonhomologous asparagines, the NR1 N site and the NR2A N+1 site (Kuner et al., 1996; Wollmuth et al., 1996) (see Fig. 7). As shown in Table 1, P_f values and P_{Ca}/P_{Cs} in channels containing substitutions of these positions, either the N site in NR1 [NR1(N0)] or the N+1 site in NR2A [NR2A(N+1)], were significantly different from those in the wild type. These results are consistent with the idea that the narrow constriction (or at minimum the M2 loop) is an important determinant of ion permeation in NMDAR channels. However, in characterizing the contribution of the narrow constriction to Ca^{2+} influx, we studied in detail only NR1–NR2A(N+1G) channels, because this mutation does not induce subconductance states (Wollmuth et al., 1998b). In contrast, substitutions of the NR1 N site do induce subconductance states, which in some instances show different permeation properties (Schneggenburger and Ascher, 1997), complicating their analysis at the macroscopic level. Finally, in contrast to the strong effects of NR1 N site substitutions, P_f values in channels containing substitutions of the NR2A N site, NR2A(N0Q) or NR2A(N0G), were not significantly different from those in the wild type.

Two highly conserved polar residues in NR1 (T630 and

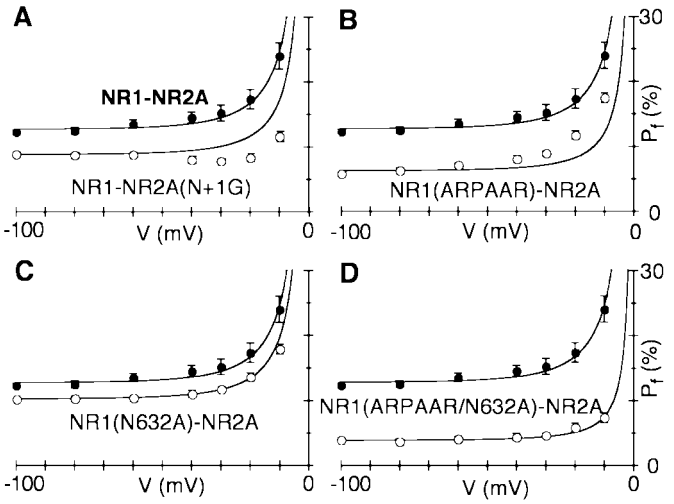

Figure 6. Voltage dependence of fractional Ca^{2+} currents. Mean P_f values measured over a wide voltage range in wild-type (●) and mutant (○) channels containing substitutions of different domains are shown. Potentials are expressed relative to the reversal potential. The *solid lines* in each plot are predicted P_f values based on the P_{Ca}/P_{Na} derived from the P_f measurement at −80 mV, using concentrations of monovalents and Ca^{2+} corrected for activity coefficients (Jatzke et al., 2002). The derived P_{Ca}/P_{Na} values are as follows: NR1–NR2A, 3.55 ± 0.06 (n = 12); NR1–NR2A(N+1G), 2.40 ± 0.08 (n = 6); NR1(ARPAAR)–NR2A, 1.68 ± 0.05 (n = 7); NR1(N632A)–NR2A, 2.85 ± 0.09 (n = 6); and NR1(ARPAAR/N632A)–NR2A, 0.96 ± 0.05 (n = 6).

N632) are also exposed to the water interface (Fig. 1). However, Ca^{2+} permeability in NR1(T630C) channels was indistinguishable from that in the wild type (Table 1). In contrast, substitutions of N632 did alter Ca^{2+} permeability, and in channels containing an alanine substitution of this position [NR1(N632A)], P_f values were significantly less than those in the wild type. Hence, Ca^{2+} influx in NMDAR channels is regulated by multiple domains, including DRPEER, the conserved asparagine (N632) in M3, and the narrow constriction of the channel.

Distinct contribution of the multiple domains to Ca^{2+} influx

Previous work has shown that the voltage dependence of P_f values in NMDAR channels depends on different parts of the pore (Schneggenburger, 1998). To further compare the contribution of the different domains to Ca^{2+} influx, we measured P_f values over a wide voltage range in wild-type and mutant NR1–NR2A channels (Fig. 6). To compare the voltage dependence of P_f values, we converted P_f values to P_{Ca}/P_{Na} and vice versa using Goldman–Hodgkin–Katz (GHK) assumptions [Jatzke et al. (2002), their Eq. 1]. We use GHK here simply as a reference point. Although P_f values are intrinsically voltage dependent, when this voltage dependency follows the GHK equation, a single P_{Ca}/P_{Na} will describe the P_f values over the entire voltage range.

For the wild type (Fig. 6*A*, ●), P_f values are described by a single P_{Ca}/P_{Na} (Fig. 6*A*, *straight line*) over the entire voltage range, as has been found previously (Schneggenburger et al., 1993; Burnashev et al., 1995). Thus, the voltage dependencies of P_f values are consistent with the predictions of the GHK equation. For NR1–NR2A(N+1G) (Fig. 6*A*, ○), P_f values are reduced relative to the wild type, but the divergence between them is greatest at intermediate potentials (−50 to −10 mV). Correspondingly, predicted P_f values (Fig. 6*A*, *straight line through open circles*), based on P_{Ca}/P_{Na} derived from the P_f measurements at −80 mV, overestimate P_f values at intermediate potentials. Thus, the voltage dependencies of P_f values deviate from GHK in a manner identical to that observed previously for other M2 loop mutations (Schneggenburger, 1998), suggesting that elements forming the narrow constriction act primarily as a permeation barrier for Ca^{2+}.

In channels in which DRPEER is neutralized (Fig. 6*B*, ○), P_f values are again attenuated over the entire voltage range relative to the wild type. However, in direct contrast to the effect of M2 loop substitutions, this attenuation is strongest at negative potentials. Hence, predicted P_f values (Fig. 6*B*, *straight line*) underestimate the measured P_f values at potentials positive to −60 mV. This pattern of P_f values is exactly opposite to that found in substitutions of the narrow constriction, indicating that DRPEER and the narrow constriction represent distinct functional elements in the process of Ca^{2+} influx.

Figure 6*C* shows that in NR1(N632A)–NR2A, P_f values are attenuated over the entire voltage range. Any effect on the voltage dependence was small. A more striking result was found for channels in which both N632 and DRPEER were neutralized [NR1(ARPAAR/N632A)–NR2A] (Fig. 6*D*, ○). P_f values in these channels were significantly reduced compared with those for the individual components and showed little voltage dependence, being described by a single P_{Ca}/P_{Na} of ~1 (Fig. 6*D*, *straight line*). Thus, these mutant channels behave as if they do not select for Ca^{2+} relative to monovalents.

DISCUSSION

Identification of external determinants of Ca^{2+} influx in NMDAR channels

Guided by sequence comparisons and structural determinants of the extracellular vestibule, we identified DRPEER, a highly charged motif located C terminal to M3 in the NR1 subunit. Initially, we identified DRPEER based on Ca^{2+} permeability measured using changes in reversal potentials. However, we characterized its properties primarily by measuring fractional Ca^{2+} currents (P_f). This approach directly quantifies Ca^{2+} influx under physiological conditions and is model independent, an important consideration given the lack of a quantitative relationship between P_f values and Ca^{2+} permeability measured using reversal potentials in GluR subtypes (Burnashev et al., 1995; Jatzke et al., 2002). In addition, channels in which DRPEER is neutralized do not show subconductance states (Fig. 4*B*) and are blocked by extracellular Mg^{2+} in a manner indistinguishable from that in the wild-type (Fig. 5), arguing against these substitutions producing a general disruption of the channel.

In NMDAR channels, a Ca^{2+} binding site of unknown molecular identity at the entrance of the pore has been proposed to contribute to their high Ca^{2+} flux rates (Premkumar and Auerbach, 1996; Sharma and Stevens, 1996). Based on P_f values, DRPEER confers high Ca^{2+} flux rates to NMDAR channels. DRPEER also displays properties consistent with its forming a binding site for Ca^{2+}: (1) Substitutions of key residues in DRPEER altered P_f values in a manner parallel to the charge neutralization (Fig. 2*A*) or inversion (Fig. 2*C*). (2) Ca^{2+} permeability, measured using changes in reversal potentials, was altered in a manner comparable with P_f values in channels containing charge neutralization (Fig. 2*B*). (3) Residues proposed to interact directly with Ca^{2+} are exposed to the water interface (Fig. 3). (4) Neutralization of DRPEER attenuates the block by extracellular Ca^{2+} at the single-channel level (Fig. 4). In NMDAR channels,

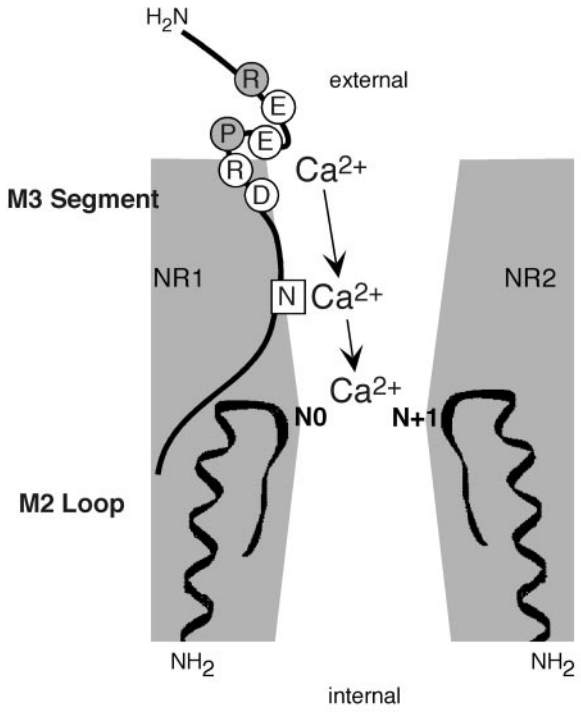

Figure 7. Multidomain model of Ca^{2+} influx in NMDAR channels. A schematic of the determinants of Ca^{2+} influx in NMDAR channels is shown. The M2 loop and M3 are indicated as *thick lines*. The narrow constriction is positioned at the approximate tip of the M2 loop and at the approximate center of the pore (Villarroel et al., 1995; Zarei and Dani, 1995). It is also formed by asparagines occupying nonhomologous positions, the NR2 N+1 site, and the NR1 N site (Wollmuth et al., 1996). Residues in DRPEER that are apparently exposed to the water interface are shown as *open circles*.

the M3 segment forms the core of the extracellular vestibule, with regions C terminal to it positioned externally and outside of the transmembrane electric field (Sobolevsky et al., 2002). Therefore, DRPEER is at a location consistent with the low voltage dependence of the proposed external Ca^{2+} site.

Residues positioned near the tip of the M2 loop, specifically those that form the narrow constriction of the channel, also contribute to Ca^{2+} influx and have been termed a deep site for Ca^{2+} (see the introductory remarks). Our results clearly demonstrate the distinction between deep and external sites for Ca^{2+} (Fig. 7). Hence, substitutions of the narrow constriction enhance the block by extracellular Ca^{2+} (Premkumar and Auerbach, 1996; Sharma and Stevens, 1996), whereas those of DRPEER attenuate it (Fig. 4), and substitutions of these domains produce exactly opposite effects on the voltage dependence of P_f values (Fig. 6*A,B*). Finally, the narrow constriction, but not DRPEER, represents a key determinant of the voltage-dependent block by extracellular Mg^{2+} (Wollmuth et al., 1998a). These results not only support the distinction between external and deep sites but also indicate that substitutions of DRPEER do not indirectly affect Ca^{2+} influx by disrupting the structure of the deep site.

The DRPEER motif as a Ca^{2+} binding site

The affinity of DRPEER for Ca^{2+} is difficult to assess directly, because Ca^{2+} can leave it via two pathways, by permeating the channel or returning to the bulk solution. Still, based on the block of wild-type channels by Ca^{2+} (Premkumar and Auerbach, 1996; Sharma and Stevens, 1996), the affinity is not great, on the order of hundreds of micromoles. DRPEER functions as a complex with all three of the negative charges, to varying degrees, contributing to the negativity required for the divalent Ca^{2+} to interact with a protein and with the positive charge at 641 acting as a countercharge for the entire motif. Based on SCAM (Fig. 3) and the lack of effect of substitutions of it on Ca^{2+} influx (Fig. 2), the side chain at R645 is apparently not exposed to the water interface. Hence, DRPEER contains at minimum a net negative charge of ~2. Nevertheless, this analysis probably underestimates the negativity of DRPEER, given that substitutions of charge residues have quantitatively different effects on Ca^{2+} influx (Fig. 2).

The mechanism of interaction of Ca^{2+} with DRPEER appears primarily to be electrostatic, with its physical shape making only a minor contribution. Indeed, substitutions of the proline in DRPEER, which functions as a structural side chain, did not have significant effects on P_f values, although they did produce a weak albeit significant effect on P_{Ca}/P_{Cs} (Fig. 2). Hence, the electrostatics of DRPEER appear to define its main binding properties.

Multidomain model of Ca^{2+} influx in NMDAR channels

Figure 7 illustrates our multidomain model of Ca^{2+} influx in NMDAR channels. In this model, DRPEER is located externally, the narrow constriction is located centrally, and the conserved asparagine, N632, is located between these two domains. Other polar residues in the NR2 M3 segment proper may also influence this process. Nevertheless, DRPEER, and to a lesser extent N632 in NR1, contribute to the high Ca^{2+} influx these channels mediate under physiological conditions. This idea is supported by the finding that channels in which DRPEER and N632 are neutralized, NR1(ARPAAR/N632A)–NR2A, no longer select for Ca^{2+} (i.e., P_{Ca}/P_{Na} is ~1) (Fig. 6*D*).

How does DRPEER, and to a lesser extent N632 in M3, increase Ca^{2+} influx? One possibility is that DRPEER acts as a surface charge, enhancing the concentration of Ca^{2+} relative to monovalents at the mouth of the pore. This seems unlikely, because surface charges do not make a significant contribution to ion fluxes in the NMDAR channel under physiological conditions (Zarei and Dani, 1994; Wollmuth and Sakmann, 1998). Alternatively, the high Ca^{2+} influx relative to monovalents may arise via a competition or exclusion mechanism, with binding of Ca^{2+} to the external site as the critical step in this process (Jahr and Stevens, 1993; Sharma and Stevens, 1996). In this scenario, when Ca^{2+} is bound to the external site, which occurs only transiently because of its low affinity for Ca^{2+}, the pore excludes monovalent ions, increasing the fraction of the total current carried by Ca^{2+}.

The block of monovalent currents by extracellular Ca^{2+} at the single-channel level (Fig. 4*A*) is consistent with an exclusion mechanism for the high Ca^{2+} influx. Nevertheless, many unresolved issues remain. One critical point is how exclusion arises given the external location of DRPEER. NMDAR channels have a single ion pore (Zarei and Dani, 1994), but DRPEER is probably positioned too externally to be within this region, which is presumably associated with the M2 loop. Alternatively, DRPEER may be located within a single file region distinct from that formed by the M2 loop. The diameter of the pore at the level of DRPEER is unknown, but if GluR subunits share a common general structure with K channels, then DRPEER would be positioned near the helical bundles formed by the second transmembrane helices and hence in a region in which the pore diameter would be relatively small. A complementary point facilitating monovalent exclusion is that Ca^{2+} may have to simulta-

neously interact with both DRPEER motifs, assuming two NR1 subunits.

The multidomain model and structural asymmetry may explain differences in Ca^{2+} permeation among GluR subtypes. Ca^{2+}-permeable AMPAR channels are approximately threefold to fourfold less efficient in carrying Ca^{2+} than NMDAR channels, having fractional Ca^{2+} currents of ~4% at −60 mV. Substituting an asparagine at the Q/R/N site of AMPAR channels, which would provide two of the three key determinants of the high Ca^{2+} influx, results in only a modest increase (1–2%) in fractional Ca^{2+} currents (Wollmuth and Sakmann, 1998). Part of the additional difference may reflect general structural differences such as subtype-specific differences in pore size, but most is presumably attributable to the absence of the DRPEER motif in non-NMDAR subunits.

Comparison with voltage-gated Ca^{2+} channels

The competition model of Ca^{2+} selectivity in NMDAR channels is reminiscent of that in voltage-gated Ca^{2+} channels (VGCCs). However, under physiological conditions, the current in VGCCs is carried exclusively by Ca^{2+}, whereas in NMDAR channels it is a mixture of monovalents and Ca^{2+}. Although both channel types have a Ca^{2+} site in the pore necessary for Ca^{2+} flux, the details of how these sites function differ in critical ways. In VGCCs (McCleskey, 1999), the binding site is of high affinity, between 0.5 and 1 μM, is located at the narrow constriction of the channel, and accommodates multiple permeant ions. All of these properties are distinct from those of the external site in NMDAR channels. Thus, the details of how the Ca^{2+} binding sites function lead to very different mechanisms of Ca^{2+} influx. In addition, high Ca^{2+} influx in NMDAR channels depends on Ca^{2+} interacting with multiple sites in the pore. This may represent a critical feature of their pores, permitting them to be both highly permeable to Ca^{2+} and blocked by extracellular Mg^{2+} in a strongly voltage-dependent manner. Thus, by distributing the process of Ca^{2+} influx throughout the pore (from the narrow constriction of the channel to the extracellular vestibule), NMDAR channels can perform a unique role in synaptic physiology: highly efficient, glutamate- and voltage-regulated influx of Ca^{2+}.

REFERENCES

Ascher P, Nowak L (1988) The role of divalent cations in the *N*-methyl-D-aspartate responses of mouse central neurones in culture. J Physiol (Lond) 399:247–266.

Beck C, Wollmuth LP, Seeburg PH, Sakmann B, Kuner T (1999) NMDAR channel segments forming the extracellular vestibule inferred from the accessibility of substituted cysteines. Neuron 22:559–570.

Burnashev N (1996) Calcium permeability of glutamate-gated channels in the central nervous system. Curr Opin Neurobiol 6:311–317.

Burnashev N, Schoepfer R, Monyer H, Ruppersberg JP, Günther W, Seeburg PH, Sakmann B (1992) Control by asparagine residues of calcium permeability and magnesium blockade in the NMDA receptor. Science 257:1415–1419.

Burnashev N, Zhou Z, Neher E, Sakmann B (1995) Fractional calcium currents through recombinant GluR channels of the NMDA, AMPA and kainate receptor subtypes. J Physiol (Lond) 485:403–418.

Dingledine R, Borges K, Bowie D, Traynelis SF (1999) The glutamate receptor ion channels. Pharm Rev 51:7–61.

Jahr CE, Stevens CF (1993) Calcium permeability of the *N*-methyl-D-aspartate receptor channel in hippocampal neurons in culture. Proc Natl Acad Sci USA 90:11573–11577.

Jatzke C, Watanabe J, Wollmuth LP (2002) Voltage and concentration dependence of Ca^{2+} permeability in recombinant glutamate receptor subtypes. J Physiol (Lond) 538:25–39.

Karlin A, Akabas MH (1998) Substituted-cysteine accessibility method. Methods Enzymol 293:123–145.

Krupp JJ, Vissel B, Heinemann SF, Westbrook GL (1996) Calcium-dependent inactivation of recombinant *N*-methyl-D-aspartate receptors is NR2 subunit specific. Mol Pharmacol 50:1680–1688.

Kuner T, Wollmuth LP, Karlin A, Seeburg PH, Sakmann B (1996) Structure of the NMDA receptor channel M2 segment inferred from the accessibility of substituted cysteines. Neuron 17:343–352.

Lee JM, Zipfel GJ, Choi DW (1999) The changing landscape of ischaemic brain injury mechanisms. Nature 399:A7–A14.

McCleskey EW (1999) Calcium channel permeation: a field in flux. J Gen Physiol 113:765–772.

Neher E (1995) The use of fura-2 for estimating Ca buffers and Ca fluxes. Neuropharmacology 34:1423–1442.

Premkumar LS, Auerbach A (1996) Identification of a high affinity divalent cation binding site near the entrance of the NMDA receptor channel. Neuron 16:869–880.

Premkumar LS, Qin F, Auerbach A (1997) Subconductance states of a mutant NMDA receptor channel kinetics, calcium, and voltage dependence. J Gen Physiol 109:181–189.

Schneggenburger R (1998) Altered voltage dependence of fractional Ca^{2+} current in *N*-methyl-D-aspartate channel pore mutants with a decreased Ca^{2+} permeability. Biophys J 74:1790–1794.

Schneggenburger R, Ascher P (1997) Coupling of permeation and gating in an NMDA-channel pore mutant. Neuron 18:167–177.

Schneggenburger R, Zhou Z, Konnerth A, Neher E (1993) Fractional contribution of calcium to the cation current through glutamate receptor channels. Neuron 11:133–143.

Sharma G, Stevens CF (1996) Interactions between two divalent ion binding sites in *N*-methyl-D-aspartate receptor channels. Proc Natl Acad Sci USA 93:14170–14175.

Sobolevsky AI, Beck C, Wollmuth LP (2002) Molecular rearrangements of the extracellular vestibule in NMDAR channels during gating. Neuron 33:75–85.

Villarroel A, Burnashev N, Sakmann B (1995) Dimensions of the narrow portion of a recombinant NMDA receptor channel. Biophys J 68:866–875.

Wollmuth LP, Sakmann B (1998) Different mechanisms of Ca^{2+} transport in NMDA and Ca^{2+}-permeable AMPA glutamate receptor channels. J Gen Physiol 112:623–636.

Wollmuth LP, Kuner T, Seeburg PH, Sakmann B (1996) Differential contribution of the NR1- and NR2A-subunits to the selectivity filter of recombinant NMDA receptor channels. J Physiol (Lond) 491:779–797.

Wollmuth LP, Kuner T, Sakmann B (1998a) Adjacent asparagines in the NR2-subunit of the NMDA receptor channel control the voltage dependent block by extracellular Mg^{2+}. J Physiol (Lond) 506:13–32.

Wollmuth LP, Kuner T, Sakmann B (1998b) Intracellular Mg^{2+} interacts with structural determinants of the narrow constriction contributed by the NR1-subunit in the NMDA receptor channel. J Physiol (Lond) 506:33–52.

Zarei MM, Dani JA (1994) Ionic permeability characteristics of the *N*-methyl-D-aspartate receptor channel. J Gen Physiol 103:231–248.

Zarei MM, Dani JA (1995) Structural basis for explaining open-channel blockade of the NMDA receptor. J Neurosci 15:1446–1454.